

Calbindin-D28k is a more reliable marker of human Purkinje cells than standard Nissl stains: A stereological experiment

Elizabeth R. Whitney^{a,*}, Thomas L. Kemper^a, Douglas L. Rosene^a,
Margaret L. Bauman^{a,b}, Gene J. Blatt^a

^a Department of Anatomy and Neurobiology, L-1004, Boston University School of Medicine,
715 Albany Street, Boston, MA 02118, United States

^b Department of Neurology, Massachusetts General Hospital, Boston, MA 02114, United States

Received 9 June 2007; received in revised form 5 September 2007; accepted 7 September 2007

Abstract

In a study of human Purkinje cell (PC) number, a striking mismatch between the number of PCs observed with the Nissl stain and the number of PCs immunopositive for calbindin-D28k (CB) was identified in 2 of the 10 brains examined. In the remaining eight brains this mismatch was not observed. Further, in these eight brains, analysis of CB immunostained sections counterstained with the Nissl stain revealed that more than 99% Nissl stained PCs were also immunopositive for CB. In contrast, in the two discordant brains, only 10–20% of CB immunopositive PCs were also identified with the Nissl stain. Although this finding was unexpected, a historical survey of the literature revealed that Spielmeyer [Spielmeyer W. *Histopathologie des nervensystems*. Julius Springer: Berlin; 1922. p. 56–79] described human cases with PCs that lacked the expected Nissl staining intensity, an important historical finding and critical issue when studying postmortem human brains. The reason for this failure in Nissl staining is not entirely clear, but it may result from premortem circumstances since it is not accounted for by postmortem delay or processing variables. Regardless of the exact cause, these observations suggest that Nissl staining may not be a reliable marker for PCs and that CB is an excellent alternative marker.

© 2007 Elsevier B.V. All rights reserved.

Keywords: Cerebellum; Purkinje cell; Nissl; Calcium binding protein; Calbindin

1. Introduction

Nissl staining procedures, developed by Franz Nissl (1860–1919), have been used extensively to study neurons in the central nervous system. In the cerebellum, Nissl stained material has been used to study several cell types, including Purkinje Cells (PCs), the output neuron of the cerebellar cortex. The data in the current paper represents an incidental, but important finding in two control brains when studying the cerebellar cortex in autism. In this study, we first determined the density of PCs in our sample of 10 brains. Additionally, we examined PC subpopulations based on calcium binding protein expression. Only the calbindin-D28k (CB) data is discussed here since, consistent with our data, CB is reportedly present in “most” human PCs (Fournet et al., 1986) and “virtually all” squirrel monkey PCs

(Fortin et al., 1998); hence, CB is an important PC marker for comparison against Nissl stained PCs.

2. Materials and methods

Cerebella that were immersion fixed in formalin were obtained from the Harvard Brain Tissue Resource Center, Kathleen Price Bryan Brain Bank at Duke University Medical Center and University of Maryland Brain Bank. Six autistic and four control brains were included in the study. All control brains were free from gross pathology and were obtained from individuals with no history of neurological disorders. Case details are shown in Table 1. All tissue sections were batch-processed in 4 groups (2 pairs, 2 triplets).

2.1. Tissue processing

In each case, a 2 cm × 2 cm × 2 cm block of tissue cut perpendicular to the folia, was obtained from the cerebellar hemisphere

* Corresponding author. Tel.: +1 617 414 2338; fax: +1 617 638 4216.
E-mail address: ewhitney@bu.edu (E.R. Whitney).

Table 1
Case Information

Case #	Group	Age	Sex	Hemisphere	PMI (h)	Years in formalin	Cause of death
Duke-495	Control	17	F	Unknown	Unknown	Unknown	Unknown
4104	Control	24	M	Left	5	Unknown	Gun Shot
4334	Control	53	M	Right	23.75	3	Cancer
BCH-13	Control	30	M	Left	Unknown	6	Unknown
4414 ^{a,b}	Autism	26	M	Left	47.68	2.5	Seizure
3845 ^{a,b}	Autism	32	M	Left	Unknown	4	Pancreatitis
4099	Autism	19	M	Left	3	4.5	CHF
4259 ^{a,c}	Autism	13	F	Left	18.36	4	Unknown
2431	Autism	54	M	Left	4	8.5	GI bleed
3511 ^{a,d}	Autism	27	M	Right	16	7.5	Trauma

Case information on autistic and control brains including: age, sex, hemisphere, postmortem interval (PMI), years in formalin and cause of death. Gastrointestinal (GI), congestive heart failure (CHF).

^a Seizure disorder.

^b History of Dilantin[®] use.

^c History of Tegretol[®] use.

^d History of Phenobarbital[®] use.

inferior to the horizontal fissure (Schmahmann et al., 2000). All tissue blocks were cryoprotected (Rosene et al., 1986) and embedded in an egg-albumin gelatin to minimize tissue damage (Crane and Goldman, 1979). They were then flash frozen in -75°C 2-methylbutane and placed in a -80°C freezer for at least 48 h before being serially sectioning on a sliding microtome. Eighteen series were cut at $30\ \mu\text{m}$ and two series were cut at $60\ \mu\text{m}$ so that sections within a series were spaced $660\ \mu\text{m}$ apart. Sections were thaw-mounted onto gelatin-subbed slides, air-dried, and stored in a -20°C freezer until the day they were stained.

In each brain, one series was Nissl stained with thionin (Fisher Chemicals, Springfield, NJ) for 2.5 min in a solution prepared at a pH of 4.2. On-the-slide series were also immunostained using specially designed wells (PolyFab Inc., Avon, MA). The optimum antibody concentration was predetermined (anti-calbindin: mouse monoclonal, 1:1000, from Swant Laboratories, Switzerland). Sections were pretreated in a 1% hydrogen peroxide solution and a blocking serum. They were then incubated in the primary antibody for 48 h followed by a 1-h incubation in a biotinylated secondary antibody (Vector Laboratories, Inc.). An avidin–biotinylated peroxidase complex solution (ABC) was then added (Vector Laboratories, Inc., Burlingame, CA) and the antigen was visualized using 3,3'-diaminobenzidine as the chromogen. Sections were air-dried overnight, lightly counterstained with thionin and coverslipped with Permount.

2.2. Purkinje cell counts

Because of the inherent differences in the Nissl stained and CB immunostained sections, counting procedures were customized accordingly. Stereological sampling principles, however, were maintained across all sections. Additionally, the same equipment was used in all counting procedures; this included a Nikon Eclipse E600 microscope (Nikon Instruments Inc., Melville, NY), Optronics DEI-750 CE camera control unit (Optronics, Goleta, CA), MAC 2002 motor stage control unit

(Ludl Electronic Products, Ltd., Hawthorne, NY) and computer software from MircoBrightField Inc. (Williston, VT).

Both Nissl stained and CB immunostained PCs were counted in nearly adjacent series of sections ($300\ \mu\text{m}$ apart). The PC layer was used as the region of interest (ROI) and, in all brains, 10 sections, equally spaced at $660\ \mu\text{m}$ intervals were counted for both stains. Within this ROI PCs were systematically sampled; the approach was based on the optical disector method (Gundersen, 1986; West et al., 1991) and ensures that all objects, regardless of size, shape and orientation, have an equal chance of being counted. Minor modifications to the counting procedure, as outline below, reflect the differences in the Nissl and CB immunostained sections; however, in all sections, the PC layer was sampled using methodology that avoided double counting in all planes.

For both stains, to avoid double counting in the z -axis, an exclusionary plane at the top of the section was implemented. This z -axis exclusionary plane was used instead of guard volumes because sections with an original thickness of $30\ \mu\text{m}$, when thaw-mounted onto slides, shrink in the z -axis to 7.5 – $8.5\ \mu\text{m}$. At this thickness and with the optics available it was not possible to implement reliable guard volumes. While this does introduce problems due to lost caps (Hedreen, 1998), the same process was used in all cases and therefore, the relative difference between sections is not affected.

For the Nissl stained sections, the nucleolus was used as the counting target as it is clearly distinguishable and prior work has shown that PCs with more than one nucleolus are rare (Nairn et al., 1989; Mayhew et al., 1990). Because the size of the PC nucleolus is relatively small, with a mean diameter of $3.6\ \mu\text{m}$ in our material, a $60\times$ oil-immersion objective lens was used to identify the nucleolus. Prior to cell counting, the length of the PC layer was measured using a $2\times$ objective lens and software from MicroBrightField Inc., Williston, VT (Stereo Investigator[®]); this measurement provided the reference length, $L(\text{ref})$, which was later used to calculate #PCs/mm. Next, the PC layer (ROI) was outlined, also using a $2\times$ objective lens and Stereo Investigator[®] software. The magnification

was then increased to a 60× oil-immersion objective lens. A 150 μm × 200 μm grid with a 75 μm × 100 μm counting frame was used to randomly and systematically sample the ROI. To avoid double counting in the *x* or *y* planes, the lower and left borders (*x* and *y*) of the counting frame as well as their extended edges were considered forbidden and PC nucleoli contacting these lines were not counted (Gundersen, 1986). The PC nucleoli within the counting frame and those contacting the upper and right borders of the counting frame were included in the counts (Gundersen, 1986). After completing the counting in one frame, the motorized stage shifted to the next counting frame. This process was repeated until all counting frames within the ROI were viewed.

The numerical density (N_v), was calculated as a ratio of the total number of PCs counted ($\sum Q$) to the total disector volume, $\sum v(\text{dis})$; the latter is determined by the number of times ($\sum P$) the disector hits the ROI reference space multiplied by the disector volume $v(\text{dis})$.

$$N_v = \frac{\sum Q}{\sum v(\text{dis})} = \frac{\sum Q}{\sum P \times v(\text{dis})}$$

The estimated total number of PCs (N) in the region of interest was then calculated as the product of N_v and the reference volume, $V(\text{ref})$. The $V(\text{ref})$ was calculated as the product of the outlined ROI (area) and section thickness.

$$N = N_v \times V(\text{ref})$$

Finally, the density of PCs (N_L) along a known length of the PC layer, $L(\text{ref})$, was calculated:

$$N_L = \frac{N}{L(\text{ref})}$$

N_L represents the number of PCs per millimeter (#PCs/mm). Data is expressed as a density measure because tissue availability did not allow us to exhaustively section the same folium across all brains.

In the CB immunostained sections, the soma was used as the counting target since the nucleus and nucleolus are often obscured by the dense immunoreaction product filling the soma. The PC soma in our material, measured 34.4 μm × 27.1 μm in height by width. As a result, PCs in these sections could be reliably counted with the 40× objective lens. This lower magnification made it feasible to count all PCs within the ROI and obtain the actual #PCs/mm rather than the estimated #PCs/mm without compromising stereological principles. First, the length of the PC layer in the region of interest was measured using a 2× objective lens. The magnification was then increased to a 40× objective lens with Nomarski optics. As with Nissl stained sections, PC somas in focus at the top of the section were excluded to prevent double counting of cells. However, along the *x* and *y* axes, the examiner viewed the entire ROI in a step-wise and systematic manner; this is possible because of the organized nature of the PC layer. Along these dimensions, the leading edge of a PC was counted when it entered the counting field. Once a PC was counted it was marked by the computer and was not at risk of being counted again. In addition to counting CB immunolabeled PCs, PCs

void of reaction product but visible with Nissl stain were also counted. The latter cells were marked as immunonegative. As with Nissl stained sections, the number of CB immunopositive PCs per unit length (N_L) was calculated and expressed as #PCs/mm.

Finally, the percentage of CB immunopositive PCs (%PC_{CB+}) was calculated as the ratio of CB immunopositive PC number (PC_{CB+}) to the total PC number (CB immunopositive and CB immunonegative) (PC_T) as follows:

$$\%PC_{CB+} = \frac{PC_{CB+}}{PC_T}$$

2.3. Statistical analysis

The paired *t*-test statistic was used to determine if a significant difference in PC density existed between Nissl stained and CB immunostained sections. Additionally, this same test was used to examine whether the postmortem interval (PMI) was significantly different in brains that stained well with thionin and those that did not.

3. Results

In 2 of 10 brains (cases 4104 and 4334) there was a paucity of Nissl stained PCs but abundant PCs on nearly adjacent CB immunostained sections (sections spaced at 300 μm) (Table 2, Figs. 1 and 2). Paired *t*-test analysis of the #PCs/mm on Nissl and CB immunostained sections revealed a statistically significant difference in these two cases with $P \leq 0.01$. In the remaining eight brains, no significant difference in PC density was observed between Nissl stained and CB immunostained sections ($P = 0.68$). Further, in these eight brains that stained well with thionin and CB, PC counts on sections CB immunostained and lightly counterstained with thionin revealed that 99.5% of PCs in the control brains and 99.4% of PCs in the autistic brains that stained with thionin were also CB immunopositive.

Table 2
Comparison of #PCs/mm in Nissl and CB stained sections

Cases	Group	Nissl (PC#/mm)	CB (PC#/mm)
Duke-495	Control	5.8	5.4
4104	Control	<u>1.2</u>	<u>5.3</u>
4334	Control	<u>0.4</u>	<u>4.0</u>
BCH-13	Control	4.4	4.0
4144	Autism	0.4	0.5
3845	Autism	2.9	2.6
4099	Autism	3.5	3.3
4259	Autism	4.0	4.3
2431	Autism	4.8	4.3
3511	Autism	5.5	5.8

Comparison of the number of PCs per millimeter in Nissl stained and CB immunostained sections in all cases (columns 3 and 4). Note the discrepancy in PC number between Nissl stained and CB immunostained sections in control cases 4104 and 4334 (bold/underlined). In brains 4104 and 4334 there is a statistically significant difference in the number of Nissl stained and CB immunostained PCs ($P < 0.01$). In the remaining eight brains, no significant difference in PC number is noted between Nissl stained and calbindin-D28k immunostained sections ($P = 0.68$).

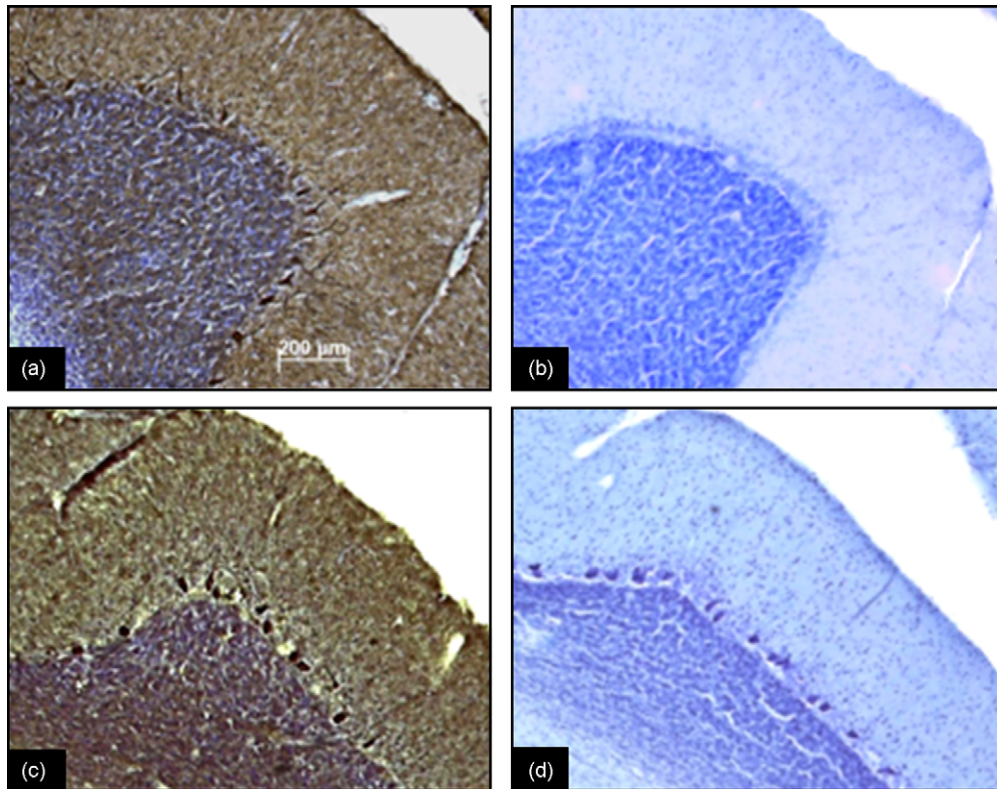


Fig. 1. Comparison of Nissl stained and Calbindin-D28k immunostained sections. (a) Control brain 4334: CB immunopositive PCs clearly visible along the PC layer; (b) control brain 4334: PCs not visible in Nissl stained sections; (c) autistic brain 3511: CB immunopositive PCs clearly visible along the PC layer; (d) autistic brain 3511: PCs clearly visible along the PC layer in Nissl stained sections. Scale bar in (a) represents 200 μm in all figures (a–d).

To determine if differences in the staining in cases 4104 and 4334 could be due to PMI or years in formalin, further analysis was performed. Using the *t*-test statistic, the PMI for cases 4104 and 4334 was compared with that of the eight well-stained

cases; this analysis revealed no statistically significant difference ($P=0.82$). Because only one of the two cases with poor Nissl staining had available data on years in formalin, statistical analysis of time in formalin could not be performed; however, one

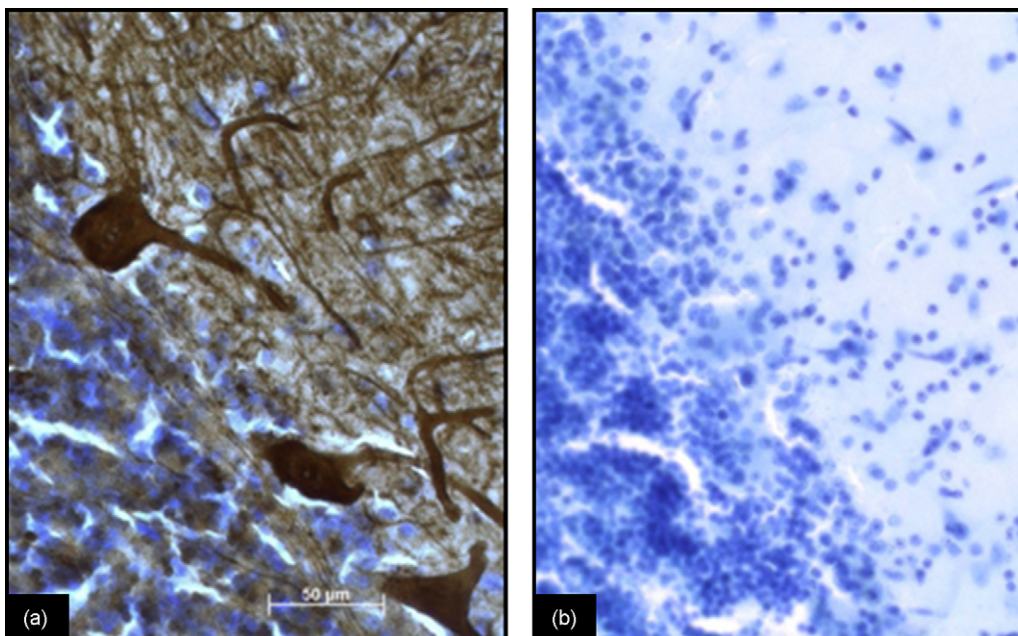


Fig. 2. Comparison of Nissl stained and Calbindin-D28k immunostained sections. (a) Control brain 4334: CB immunopositive PCs clearly visible along the PC layer; (b) control brain 4334: PCs not visible on Nissl stained section. Scale bar in (a) represents 50 μm in (a and b).

of these cases, 4334, had one of the shortest periods in formalin (3 years) and thus, it seems unlikely that this could account for the anomalous staining in this case.

Because of the staining issue, a spare series from these two brains were stained with variations on the standard thionin protocol as follows: (1) sections remained in thionin from one to 48 h, (2) the pH of the dH₂O wash carried out immediately prior to immersion in thionin was increased to 8.0, 8.5, 9.0, 9.5, and 10.0 and (3) the pH of the thionin was increased from 4.2 to 5.2. These modifications did reveal additional PCs, but the staining remained inadequate for stereology as the PC soma was very pale in appearance and the nucleolus often not visible (Fig. 3). Additionally, to ensure that the staining issue was not specific to thionin, spare sections were Nissl stained with cresyl violet (Chroma-Gesellschaft, Germany). The staining of PCs in these sections remained inadequate for accurate PC counts. This indicates that the stain and/or staining technique were not problematic. These data indicate that CB provides a more reliable marker for total PC number than standard Nissl staining.

4. Discussion

4.1. Thionin staining

An unexpected finding was the failure of thionin to reliably stain PCs in 2 of the 10 brains. Relative to the number of PCs stained with CB, only 10% of PCs in case 4334 and 20% of PCs in case 4104 were Nissl stained. Extensive modifications of the thionin staining protocol failed to rectify this situation, suggesting that it was not an artifact of the staining technique. Furthermore, inadequacy of the Nissl stain is specific to PCs. The latter point is clearly illustrated in Fig. 3, which reveals the marked contrast in staining intensity in adjacent cerebellar cell types.

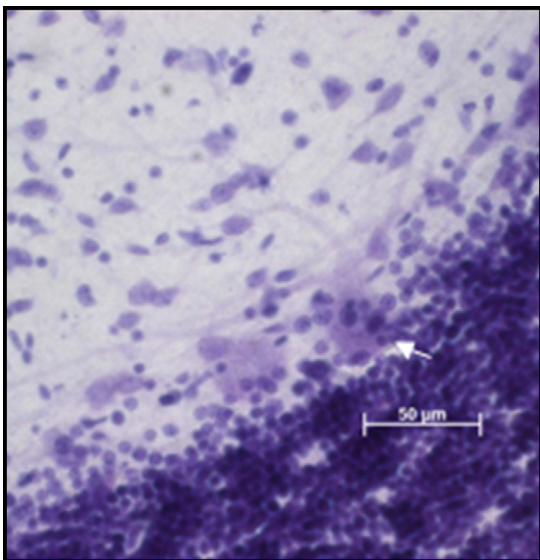


Fig. 3. Modified thionin stained sections in control brain 4334: pH of water 10.5 prior to placing sections in thionin; sections remained in thionin \times 48 h. Staining of PCs is enhanced but remains suboptimal (arrow). Note the contrast in staining intensity in the granule cells (intensely stained) compared with the PCs (lightly stained). Scale bar represents 50 μ m.

Consistent with our findings, Spielmeier (1922) was the first to describe cases with deficient PC Nissl staining properties. Using postmortem human tissue, he identified cases in which Nissl stained PCs were uncharacteristically pale and homogenous in appearance; this observation was in contrast other cerebellar cell types, which stained with normal intensity. Based on case histories, Spielmeier suggested that the altered staining intensity might be associated with fever, infection or general disease. Hypoglycemia (Lawrence et al., 1942) and ischemia (Blackwood et al., 1963) were later identified as possible causes for the pale appearance of Nissl stained PCs in human cases.

In the current study, the cases with insufficient PC Nissl staining (4101 and 4334) died from a gun shot wound and cancer, respectively. While available records do not provide specific data, both cases may have been associated with a prolonged hypoxic agonal state. PCs are particularly vulnerable to ischemia (Cervos-Navarro et al., 1991; Welsh et al., 2002) and associated calcium-mediated excitotoxicity (Brorson et al., 1995; Mishra and Delivoria-Papadopoulos, 1999). Further, accumulation of intracellular Ca²⁺ ions has been associated with increased H⁺ ion levels (Hartley and Dubinsky, 1993); this acidic environment may diminished the thionin–nucleic acid electrostatic linkage and negatively impact thionin staining. In our modified thionin staining procedure, the increase in pH of the dH₂O together with the prolonged exposure to thionin, did reveal additional PCs; however, the enhanced staining was insufficient for accurate cell counting. We suggest that the enhanced PC staining may have been related to the displacement of H⁺ ions from the nucleotide binding site thus, exposing these sites to the chromophore. Conversely, the failure of these PCs to stain with normal intensity may, in part, be the result of DNA and/or RNA degradation, which has been suggested to be associated with the acidosis that accompanies the hypoxic agonal state (Katsetos et al., 2001; Ross et al., 1992; Kingsbury et al., 1995). While this is a plausible hypothesis, altered Nissl staining has not been identified in a rodent model of hypoxia (Katsetos et al., 2001). Thus, the cause for the altered staining properties in human PCs may be more complex than the effect ischemia alone and, additional unknown factors may also have contributed to this finding.

PMI must also be considered when using human tissue; however, the inadequate Nissl staining in cases 4104 and 4334 cannot be fully explained by PMI. Although case 4334 did have one of the longer PMIs (23.75 h), case 4104, had one of the shortest PMIs (5 h). Similarly, our data does not directly point to the length of time in formalin since case 4334 was at the lower range (2.5–8.5 years) of our cases, with only 3 years in formalin. The time in formalin for case 4104 is unknown.

In summary, while the cause of the poor Nissl staining in two cases is unknown, these observations highlight the vulnerability of PCs and suggest extreme caution in interpreting PC counts based solely on Nissl stained material. Further, this work finds that CB is an excellent alternative marker for human cerebellar PCs with more than 99% of PCs identified in well-stained Nissl material also being immunopositive for CB, a finding that is in general agreement with previous work (Fournet et al., 1986; Fortin et al., 1998).

Acknowledgements

We thank Michael Bowley who was instrumental in stereology software instruction and maintenance of the system. We are also grateful to several members of the laboratory for their assistance with tissue processing: Rita Marcon, Sandy Thevarkunnel, Matthew Stoker, Melissa Martchek and Matthew Fields. This work was supported by NIH-NICHHD HD39459, National Alliance for Autism Research (NAAR), the Nancy Lurie Marks Foundation and a grant from the John and Lisa Hussman Foundation.

References

- Blackwood W, McMenemey WH, Meyer A, Norman RM, Russell DS. Greenfield's neuropathology. Baltimore: William and Wilkins; 1963. p. 29–34.
- Brorson JR, Manzillo PA, Gibbons SJ, Miller RJ. AMPA receptor desensitization predicts the selective vulnerability of cerebellar Purkinje cells to excitotoxicity. *J Neurosci* 1995;15:4515–24.
- Cervos-Navarro J, Sampaolo S, Hamdorf G. Brain changes in experimental chronic hypoxia. *Exp Pathol* 1991;42:205–12.
- Crane AM, Goldman PS. An improved method for embedding brain tissue in albumin-gelatin. *Stain Technol* 1979;54:71–5.
- Fortin M, Marchand R, Parent A. Calcium-binding proteins in primate cerebellum. *Neurosci Res* 1998;30:155–68.
- Fournet N, Garcia-Segura LM, Norman AW, Orci L. Selective localization of calcium-binding protein in human brainstem, cerebellum and spinal cord. *Brain Res* 1986;399:310–6.
- Gundersen HJ. Stereology of arbitrary particles. A review of unbiased number and size estimators and the presentation of some new ones, in memory of William R. Thompson. *J Microsc* 1986;143:3–45.
- Hartley Z, Dubinsky JM. Changes in intracellular pH associated with glutamate excitotoxicity. *J Neurosci* 1993;13:4690–9.
- Hedreen JC. Lost caps in histological counting methods. *Anat Rec* 1998;250:366–72.
- Katsetos CD, Spandou E, Legido A, Taylor ML, Zanelli SA, de Chadarevian JP, et al. Acute hypoxia-induced alterations of calbindin-D28k immunoreactivity in cerebellar Purkinje cells of the guinea pig fetus at term. *J Neuropathol Exp Neurol* 2001;60:470–82.
- Kingsbury AE, Foster OJ, Nisbet AP, Cairns N, Bray L, Eve DJ, et al. Tissue pH as an indicator of mRNA preservation in human post-mortem brain. *Brain Res Mol Brain Res* 1995;28:311–8.
- Lawrence RD, Meyer a, Nevin S. The pathological changes in the brain in fatal hypoglycaemia. *Quart J Med* 1942;35:181–201.
- Mayhew TM, MacLaren R, Henery CC. Fractionator studies on Purkinje cells in the human cerebellum: numbers in right and left halves of male and female brains. *J Anat* 1990;169:63–70.
- Mishra OP, Delivoria-Papadopoulos M. Cellular mechanisms of hypoxic injury in the developing brain. *Brain Res Bull* 1999;48:233–8.
- Nairn JG, Bedi KS, Mayhew TM, Campbell LF. On the number of Purkinje cells in the human cerebellum: unbiased estimates obtained by using the “fractionator”. *J Comp Neurol* 1989;290:527–32.
- Rosene DL, Roy NJ, Davis BJ. A cryoprotection method that facilitates cutting frozen sections of whole monkey brains for histological and histochemical processing without freezing artifact. *J Histochem Cytochem* 1986;34:1301–15.
- Ross BM, Knowler JT, McCulloch J. On the stability of messenger RNA and ribosomal RNA in the brains of control human subjects and patients with Alzheimer's disease. *J Neurochem* 1992;58:1810–9.
- Schmahmann JD, Doyon J, Toga AW, Petrides M, Evans AC. MRI Atlas of the human cerebellum. San Diego: Academic Press; 2000. p. 3–20.
- Spielmeyer W. Histopathologie des nervensystems. Berlin: Julius Springer; 1922. p. 56–79.
- Welsh JP, Yuen G, Placantonakis DG, Vu TQ, Haiss F, O'Hearn E, et al. Why do Purkinje cells die so easily after global brain ischemia? Aldolase C, EAAT4, and the cerebellar contribution to posthypoxic myoclonus. *Adv Neurol* 2002;89:331–59.
- West MJ, Slomianka L, Gundersen HJ. Unbiased stereological estimation of the total number of neurons in the subdivisions of the rat hippocampus using the optical fractionator. *Anat Rec* 1991;231:482–97.